ORIGINAL ARTICLE

Synthesis of gold nanoparticles using *Sambucus wightiana* extract and investigation of its antimicrobial, anti-inflammatory, antioxidant and analgesic activities

Fazli Khuda [a,*], Zafar Ul Haq [a], Ihsan Ilahi [a], Rahim Ullah [a], Ayub Khan [b], Hassan Fouad [c], Atif Ali Khan Khalil [d,e], Zaki Ullah [a], Muhammad Umar Khayam Sahibzada [f], Yasar Shah [g], Muhammad Abbas [g], Tayyaba Iftikhar [g], Gaber El-Saber Batiha [h]

[a] *Department of Pharmacy, University of Peshawar, Peshawar, Pakistan*
[b] *Department of Chemistry, University of Education, Jauharabad Campus, Lahore, Pakistan*
[c] *Applied Medical Science Department, Community College, King Saud University, Riyadh, Saudi Arabia*
[d] *Department of Biological Sciences, National University of Medical Sciences, Rawalpindi, Pakistan*
[e] *College of Pharmacy and Research Institute of Pharmaceutical Sciences, Gyeongsang National University, Jinju, Korea*
[f] *Department of Pharmacy, Sarhad University of Science and Information Technology, Peshawar, Pakistan*
[g] *Department of Pharmacy, Abdul Wali Khan University, Mardan, Pakistan*
[h] *Department of Pharmacology and Therapeutics, Faculty of Veterinary Medicine, Damanhour University, Damanhour, AlBeheira, Egypt*

Abstract Resistance to antimicrobial agents are rendering therapies ineffective around the globe, leading to increased mortality and treatment cost. Likewise, non-steroidal anti-inflammatory drugs (NSAIDs) and analgesics possess several side effects particularly peptic ulcer and gastrointestinal problems. Metallic nanoparticles significantly enhances the therapeutic efficacy of natural extracts owing to improved bioavailability thereby lowering the dose and side effects. The purpose of this research was to investigate the efficacy of gold nanoparticles (AuNPs). In this study, *Sambucus wightiana* whole plant aqueous extract was used for rapid and eco-friendly synthesis of AuNPs.

* Corresponding author.
E-mail addresses: fazlikhuda@uop.edu.pk (F. Khuda), menhfef@ksu.edu.sa (H. Fouad).
Peer review under responsibility of King Saud University.

Production and hosting by Elsevier

They were characterized by various analytical techniques including UV–Visible spectroscopy (UV–Vis), transmission and scanning electron microscopy (TEM and SEM), energy dispersive X-ray spectroscopy (EDX), Zetasizer, X-ray diffractometer (XRD) and Fourier transform infra-red spectroscopy (FTIR). The UV–*Vis* spectra revealed a distinct absorption peak at 539 nm; TEM and SEM images confirmed the formation of heterogeneously dispersed AuNPs with an average area of 152.77 nm^2 and width of 15.96 nm. The AuNPs showed significant inhibitory zones against *Escherichia coli* (25 mm), *Staphylococcus epidermis* (23 mm) and *Salmonella enteritidis* (18 mm) with MIC values 0.13, 0.11 and 0.16 mg/ml, respectively. Among fungal strains it showed highest percent inhibition against *Fusarium* solani (90%) and *Microsporum* canis (80%) with MIC values 0.02 and 0.01 mg/ml, respectively. It showed maximum anti-inflammatory activity (43.70, 48.80 and 57.08%) at 20 mg/kg dose at both early and late hours of inflammation. Likewise, *in vitro* models depicted concentration dependent inhibition of 5-LOX and COX-2 enzymes. AuNPs showed highest antioxidant activity (68.7% inhibition) at 1000 μg/ml, compared to ascorbic acid that showed 77.8% inhibition at the same concentration. Similarly, it exhibited significant (P ≤ 0.001) dose dependent analgesic effect with maximum inhibition (56.22%) at 20 mg/kg. In conclusion, the above findings suggest that AuNPs should be studied further in order to develop safe and effective formulations.

1. Introduction

Green synthesis has received a lot of attention in recent decades due to its numerous advantages over other methods of nanoparticle synthesis. It offers several benefits such as the use of environment friendly solvents and nontoxic chemicals (Tejasvi et al., 2021). This method make use of natural agents including phytochemical such as alkaloids, flavonoids, steroids and proteins as a reducing agents which converts metal salts into metallic nanoparticles; contrary to chemical methods that involve the use of surfactants and organic solvents as reducing agents (Ihsan et al., 2021). These latter methods produce toxic by-products and necessitate stringent conditions, making them risky and costly (Dan et al., 2020). Hence, green synthesis may be considered as an alternative approach for the rapid and safe synthesis of metallic nanoparticles. Because of their widespread practical application in fields such as biomedicines, chemical sensors, targeted drug delivery, drug-gene delivery, and biomedical sciences, gold nanoparticles have recently received rigorous attention (Lydia et al., 2020; Tokeer et al., 2013). It has been used for its anticancer, antioxidant, antimicrobial, anti-inflammatory and wound healing properties (Kar et al., 2020; Muhammad et al., 2017; Sundus, and Bin, 2020).

Sambucus wightiana Wall. ex Wight & Arn. (Adoxaceae) is one of the widely distributed perennial woody shrub in subcontinent. In Pakistan, it mostly grows in the hilly areas such as Kalam and Swat (Niaz et al., 2019). This plant contains a variety of phytochemicals such as flavonoids, polyphenols, steroids, and glycosides (Khafsa et al., 2018). In folk medicines, it has been used to treat a variety of pathological conditions such as inflammation, skin infection, urinary tract infection (UTI), enteritidis, typhoid, cancer and hypertension (Chashoo et al., 2012; Najamul et al., 2020; Niaz et al., 2019). The biological activities of *S. wightiana* revealed that the phenolic and flavonoid contents are mainly responsible for its analgesic, anticancer, anti-inflammatory and antimicrobial activities (Mudasir et al., 2018; Najamul et al., 2020). Because of the plant's wide range of therapeutic applications, biosynthesis of AuNPs from it may improve its safety and efficacy.

Herein, we describe a green method to fabricate AuNPs using *S. wightiana* whole plant extract as natural reducing and stabilizing agent. The physical characterization of AuNPs were carried out using UV–Vis spectroscopy, EDX, XRD, TEM, SEM, FTIR, and Zetasizer. The synthesis of AuNPs was optimized in respect of various parameters such as temperature and pH. Subsequently, the antimicrobial, antioxidant, anti-inflammatory, and analgesic potential of the AuNPs were assayed using *in vitro* and animal models.

2. Material and methods

2.1. Plant material processing

S. wightiana was collected from district Swat (Kalam valley), Khyber Pakhtunkhwa (KPK), Pakistan (Specimen number F.Khuda-32521). The plant was thoroughly washed with deionized water (DI), dried in the shade, ground into powder, and then stored in polythene bags for future use.

2.1.1. Preparation of plant extract

The method of Ahmad et al. was followed for the preparation of aqueous extract (Ahmad et al., 2017). The powdered material (50 g) was soaked in DI water (500 ml) and heated (50–55 °C) for 30 min. The extract was then stirred (400 rpm) for 1 h. followed by centrifugation (7000 rpm) for 10 min. The supernatant was filtered on Whatman No. 1 filter paper and the clear filtrate was kept at 4 °C.

2.2. Gold nanoparticles synthesis

AuNPs were synthesized using an established procedure (Alaa et al., 2018). In a typical experiment, 100 ml aqueous tetrachloroauric acid trihydrate ($HAuCl_4 \cdot 3H_2O$) solution (2 mM) was prepared in an Erlenmeyer flask. Then 1, 2, 4, and 5 ml of extract was separately added to gold solution (10 ml; 2 mM) and stirred (350 rpm) at room temperature for at least 1 h. The procedure was carried out in a dark chamber in order to prevent photooxidation. The dark-green solution rapidly changed to ruby-red, indicating the formation of AuNPs as a

result of reduction of the salt to its elemental form. The mixture was incubated (37 °C) for 24 h in order to maximise AuNPs synthesis. Reduction of gold salt to AuNPs was monitored by recording the UV–vis absorption spectrum as a function of time.

2.2.1. Purification of gold nanoparticles

The AuNPs were centrifuged (12,000 rpm) for 10 min. To remove any unreacted moieties and free ions, the nanoparticles were washed with deionized water. They were then washed with distilled ethanol and dried on a freeze drier. The dried pellets were kept at 25 °C for subsequent analysis and biological applications (Ahmad et al., 2017).

2.3. Physical characterization

The initial synthesis of nanoparticles was confirmed by analyzing the Surface plasmon resonance (SPR) peaks using UV–*Vis* spectrophotometry (Perkin-Elmer, Lambda 35, Germany). The surface morphologies were analyzed with SEM (S-2500, Japan) and TEM (Hitachi-7650, Japan). The elemental composition of AuNPs was analysed using EDX (NOVA-450 instrument) while its crystallinity was confirmed by XRD (JDX-3532 JEOL, Japan). FT-IR (Version 10.5.1, Perkin-Elmer) was used to investigate various moieties that could help with the synthesis and capping of AuNPs. The Zetasizer was used to determine the zeta size/potential of nanoparticles.

2.4. Stability and optimization of AuNPs

The effect of substrate concentrations, pH, and temperature on AuNPs synthesis was optimised. The pH was optimised by dispersing it in phosphate buffer at 3, 5, 7, 9, and 13 pH ranges. Temperature base optimization was carried out by combining $HAuCl_4\cdot 3H_2O$ and plant extract at increasing temperatures of 20, 40, 60, and 80 °C. To analyze the effect of different concentrations of substrate on the synthesis of AuNPs, fixed volume of plant extract was mixed with $HAuCl_4\cdot 3H_2O$ solution (1:5, 1:9, 1:13, and 1:17 v/v, respectively) and optimum concentration was determined using UV–Vis spectroscopy. The stability of SPR peaks was evaluated over a 60-day study period.

2.5. In vitro studies

2.5.1. Bacterial strains

Antibacterial activity was performed against the following strains: *Bacillus subtilis* (ATCC 6633), *Shigella flexneri* (ATCC 29903), *Escherichia coli* (ATCC 5922), *Pseudomonas aeruginosa* (ATCC 27853), *Salmonella typhi* (ATCC 19430), *Salmonella enteritidis* (ATCC 13076), *Staphylococcus aureus* (ATCC 25923) *Staphylococcus epidermidis* (ATCC 12228), and *Klebsiella pneumonia* (ATCC 700603).

2.5.1.1. Agar-well diffusion method. The method of Boyanova et al. was used for the preparation of microbial cultures (Boyanova et al., 2005). They were grown in sterile Muller Hinton Agar (MHA) using sterile petri dishes. Microbial cultures with different strains (100 µl) were added to MHA (100 ml) and poured into specified petri dishes. Well for both

sample and control were made into each agar plate using sterile cork borer. 3 mg of plant extract and or/ AuNPs were dissolved in DMSO (3%; 1 ml), and 100 µl of sample was transferred into the 6 mm wells. The plates were then incubated for 48 h at 37 °C. Finally, zone of inhibition was measured using a ruler (n = 3). Imipenem was used as positive control.

2.5.2. Fungal strains

Antifungal activity was conducted against the following strains: *Candida glabrata* (ATCC 90030), *Fusarium solani* (ATCC 11712), *Aspergillus flavus* (ATCC 32611), *Trichophyton longifusis* (Clinical isolate), *Aspergillus terreus* (ATCC 20542), *Alternaria alternata* (ATCC 96154), *Candida albicans* (ATCC 2091), *Aspergillus niger* (ATCC 10549) and *Microsporum canis* (ATCC 11622).

2.5.2.1. Agar slanting method. The studied fungal strains were cultured on Sabouraud dextrose agar (SDA) and incubated at 37 °C for 24 h. The inoculum were poured into sterilized test tubes containing 4 ml of SDA. The test sample was made by dissolving 25 mg in 1 ml of 3% DMSO. In each test tube containing SDA, approximately 65 µl of the sample was added. The media was solidified and incubated (37 °C) for seven days. Miconazole and DMSO were used as positive and negative controls, respectively (Fazli et al., 2012). After incubation, the linear growth inhibition was determined and percent inhibition was calculated using Eq. (1).

$$\% \text{ inhibition} = 100 - \frac{\text{Linear growth (test)}}{\text{Linear growth (control)}} \times 100 \qquad (1)$$

2.5.3. Minimum inhibitory concentration (MIC)

The MIC was determined using 96 well microtiter plates and a micro-dilution procedure (Eloff, 1998). Under laminar flow conditions, the test sample was dissolved in DMSO and serially diluted with sterile water (to obtain various dilutions ranging from 0.1 to 30 mg/mL) in microtiter plates. After that, test growing cultures (1.5108 cfu/ml) of susceptible strains were added to different wells and incubated (37 °C) for 24 and 72 h, respectively for bacteria and fungi. Tetrazolium salt was added to each well and the violet color of the culture indicated the growth of organisms. Imipenem and miconazole served as standards, with DMSO serving as a negative control. The MIC was determined by taking the lowest concentration of the test solution that inhibited growth.

2.5.4. Cyclooxygenase (COX-2) assay

The In vitro enzyme inhibition activity was determined using the previously described method (Olomola et al., 2020). The co-factor (50 µl) and enzyme (300 U/ml) solutions were preincubated for 10 min on ice. Moreover, 50 µl of co-factor solution (1 mM hematin, 0.24 mM *N,N,N,N*-tetramethyl-*p*-phenylenediamine dihydrochloride (TMPD) and 0.9 mM glutathione in 0.1 M Tris HCl buffer with pH 8.0) was added to the enzyme solution. Likewise, the enzyme-solution (60 µl) and AuNPs (20 µl) or extract (15.6–1000 µg/mL) were kept at 25 °C for five min. For initiation of reaction 20 µl of 30 mM arachidonic acid was added to the mixture followed by incubation for 4 to 5 min. Finally, the absorbance was measured at 570 nm with a UV–*vis* spectrophotometer.

2.5.5. 5-lipoxygenase (5-LOX) assay

AuNPs, extract and standard Montelukast solutions were prepared at various concentrations (15.6–1000 µg/ml). In addition, phosphate buffer (50 mM, pH 6.3) and 5-LOX enzyme solution (10,000 U/ml) were prepared. Test samples were dissolved in phosphate buffer (250 µl) and 5-LOX (250 µl) solution was added to it followed by incubation at 25 °C for 5 min. Furthermore, Linoleic-acid (0.6 mM, 1 ml) and enzyme solutions were mixed and maximum absorbance determined at 234 nm (Okur et al., 2021). Eq. (2) was used for calculation of percent inhibition values.

$$Percent\ Inhibition = \frac{Control\ Absorbance - Sample\ Absorbance}{Control\ Absorbance} \times 100 \qquad (2)$$

2.5.6. DPPH free radical scavenging assay

This assay was carried out in accordance with the published method, with minor modifications (Ahmad et al., 2020). The 1,1-diphenyl,2-picrylhydrazyl (DPPH) (4 mg) was dissolved in 100 ml methanol to obtain 0.01 mM DPPH solution. The stock solutions of the test samples (AuNPs and extract; 1 mg/ml each) were prepared in methanol and different concentrations (15.6–1000 µg/ml) were made from it. From each concentration, 100 µl was added to 3 ml DPPH in methanol. After 15 min. of incubation at 23 °C the absorbance was measured at 517 nm. In this activity, ascorbic acid was used as a standard drug. The IC_{50} values were calculated using Graphpad prism software. The percentage DPPH radical scavenging potential was measured using Eq. (3).

$$\%\ Radical\ scavenging\ potential = \frac{C_{Abs} - S_{Abs}}{C_{Abs}} \times 100 \qquad (3)$$

where C_{Abs} and S_{Abs} are the absorbance of the control and test samples/standard, respectively.

2.6. In vivo studies: anti-inflammatory and analgesic activities

2.6.1. Animals

Male and female healthy BALB/c mice (avg. wt. 25–30 g) were provided by the Department of Pharmacy, University of Peshawar and were kept in metal cages for seven days (22 ± 2 °C and a 12 h light/dark cycle). They had free access to food and water *ad libitum*. The institutional Ethical Committee approved the study protocol under application number 09/EC/F.LIFE-2020.

2.6.2. Carrageenan-induced paw edema

The anti-inflammatory activity was determined using a well-established method (Lingadurai et al., 2007). Eight groups of 5 animals were treated with *S. wightiana* (50,100 and 200 mg/kg), AuNPs (5, 10 and 20 mg/kg), diclofenac (20 mg/kg) and normal saline. The nanoparticles and plant extract were given intraperitoneally (ip). Paw edema was induced thirty min. after the administration of the tested agents with a carrageenan solution (0.05 ml; 1%) injected into the left hind paw's subplantar region. The linear paw circumference was measured using digital plethysmometer (Plan lab, Spain). Measurements were made at different time intervals; immediately before the injection of carrageenan

and at 1, 2 and 5 h. Percentage inhibition was measured using Eq. (4)

$$\%Inhibition = \left(\frac{C - T}{C}\right) \times 100 \qquad (4)$$

where T and C represent the test and control treatment groups' increases in paw volume, respectively.

2.6.3. Hot plate test (central analgesic activity)

The method of Winter et al. (1962) was followed for this test (Winter et al., 1962). The hot plat test was carried out at a temperature of 54 ± 0.1 °C. Eight groups of 5 animals (BALB/c mice, avg. wt. 20 g) were treated with AuNPs (5, 10 and 20 mg/kg), *S. wightiana* (50,100 and 200 mg/kg), tramadol (20 mg/kg) and normal saline. The nanoparticles and plant extract were given intraperitoneally (ip). Post-treatment cut-off time was set at 30 s. The animals were subjected to a hot plate thirty min. after receiving the drug and the reaction time e.g. the time it took for the animal to jump or to lick its paw from the hot plate was recorded at 30, 60 & 90 min. of drug administration. Eq. (5) was used to compute the percentage protection (PT).

$$PT = \left(\frac{Tl - Cl}{Ct - Cl}\right) \times 100 \qquad (5)$$

where Ct: cut off time; *Tl*, *Cl*: test and control latencies, respectively.

2.7. Statistical analysis

One-way ANOVA along with Dunnet post hoc test was used for statistical analysis. (GraphPad Software Inc., San Diego, California, USA). The data were presented as mean ± SEM (n = 5).

3. Results and discussion

3.1. AuNPs synthesis

The addition of a 2 mM $HAuCl_4 \cdot 3H_2O$ solution changed the color of plant extract from green to ruby red. The rapid synthesis of AuNPs indicates presence of compounds such as alkaloids, glycosides, tannins, flavonoids etc which may be involved in the reduction of gold salt to its elemental form and subsequently to AuNPs. The present method of nanoparticles synthesis is comparatively simple, less time consuming and safe as compared to previously published methods.

3.2. Characterization of AuNPs

SEM and TEM images were used to determine the surface and internal morphological features of AuNPs. The SEM image (Fig. 1A) indicates the formation of heterogeneously dispersed AuNPs. TEM images (Fig. 1B, 1C, and 1D) further explore that AuNPs have variable sizes and different shapes. The common shapes observed were trigonal, cubic, hexagonal, and polygonal, with an average width of 15.96 nm and area of 152.77 nm^2 (Fig. S1A & B). The formation of poly-dispersed
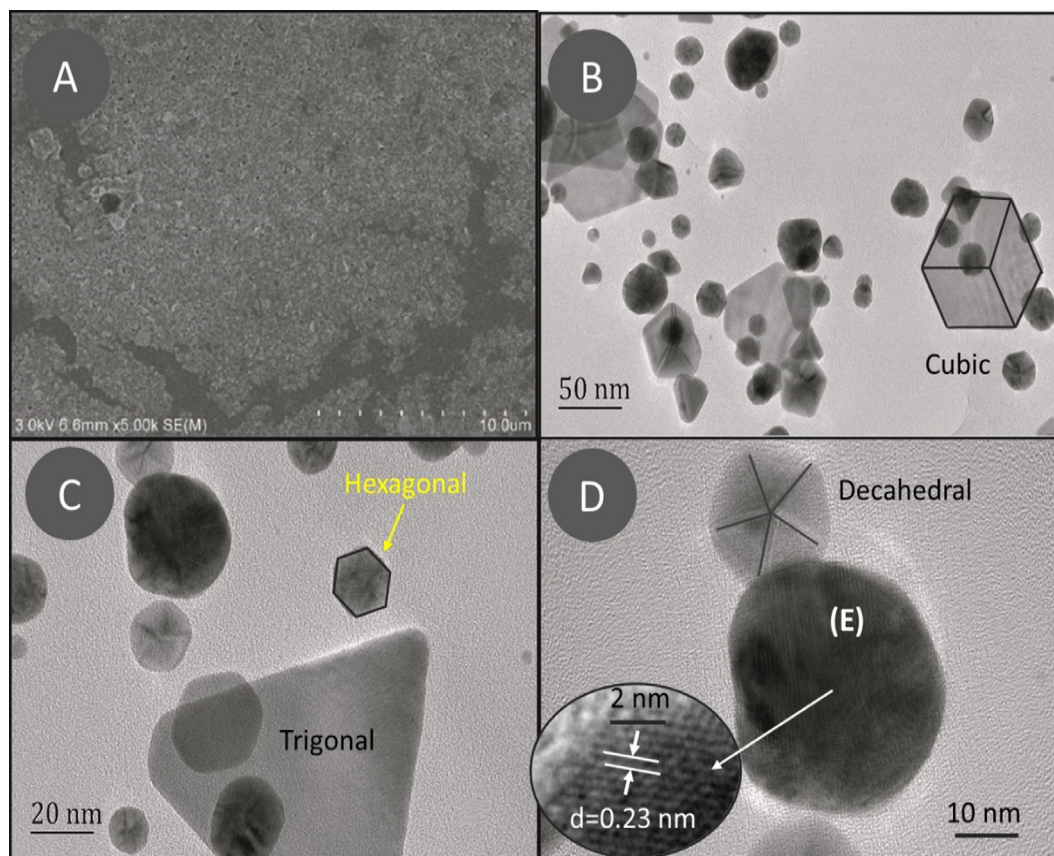
Fig. 1 (A) SEM and (B, C, and D) TEM images of AuNPs at various resolutions.

AuNPs were due to the early & later stages of nucleation. The HRTEM study discloses the single crystalline nature of AuNPs that have a common geometry of face centered cubic structure with interlayer spacing equal to 2.3 Å (Suh et al., 1998). Furthermore, Fig. 1D reveals the formation of fivefold twisted structures which confirms the existence of decahedral shapes (Elechiguerra et al., 2006; Niu, and Xu, 2011). In Fig. 1D, the particle labeled as (E) presents an image of the AuNPs with enhanced structural order.

Fig. 2A depicts the UV–vis spectra of extract and AuNPs in the wavelength range 350 to 800 nm. The absorption peak (surface plasmon resonance) of AuNPs, was observed at a wavelength of 539 nm.

The XRD pattern (Fig. 2B) revealed the characteristic peaks at 2θ values of 38.1°, 44.3°, 64.5°, and 77.7°, which respectively, related to standard Bragg reflections of (1 1 1), (2 0 0), (2 2 0), and (3 1 1) plain of the face centered cubic structure of AuNPs (JCPDS file: 040784). With a lattice parameter of α = 4.22 Å and a crystallite size of 14.2 nm, the zero valent gold crystal grows in the (1 1 1) direction, as demonstrated by the abrupt intensity peak at 38.1°.

The energy dispersive X-ray analysis (EDX) was performed using a 200-kV electron beam, to carry out the elemental analysis. Fig. 2C carries an intense Au-peak which confirms the presence of Au in the sample. The EDX spectrum also contained peaks for other elements such as C, O, and Cu. These peaks (for C, O, and Cu) are due to capped biomolecules and a carbon coated copper grid, respectively. The absence

of any other peaks demonstrates the high purity of the synthesised AuNPs. However, the presence of Si in the spectrum is because of the glass slide that holds the AuNPs.

The FT-IR spectrum of extract and AuNPs confirms the presence of various functional groups (Fig. 2D). These functional groups are important in the stabilisation and capping of Au ions. The hydroxyl group is responsible for the absorption bands at 3251.03 cm^{-1}; C = C and N-O stretching's are responsible for the peaks at 1602.94 and 1373.64 cm^{-1}, respectively. Similarly, the bands at 1047.81 cm^{-1} and 824.32 cm^{-1} correspond to C–N and C = N stretching vibration, respectively.

Zetasizer was used to determine the zeta potential and size of AuNPs (Malvern). The zeta potential and size were determined to be −37.2 mV and 230 nm, respectively (Fig. S2A & B).

3.3. Optimization of AuNPs

Fixed volume of plant extract was treated with variable volume of gold salt solution using the following ratios; 1:5, 1:7, 1:9, 1:13, and 1:15 v/v, respectively. Optimum synthesis was observed at 1:15 v/v (Fig. 3A). AuNPs showed maximum absorption at neutral and acidic pH. It was observed that the SPR peaks diminished at basic pH which reveals that the AuNPs are stable at neutral and acidic pH (Fig. 3B). The stability of AuNPs were also assessed at variable temperatures of 20, 40, 60, and 80 °C. AuNPs showed maximum absorption at 80 °C with absorption band at 528 nm (Fig. 3C). Further, the stability of nanoparticles were evaluated
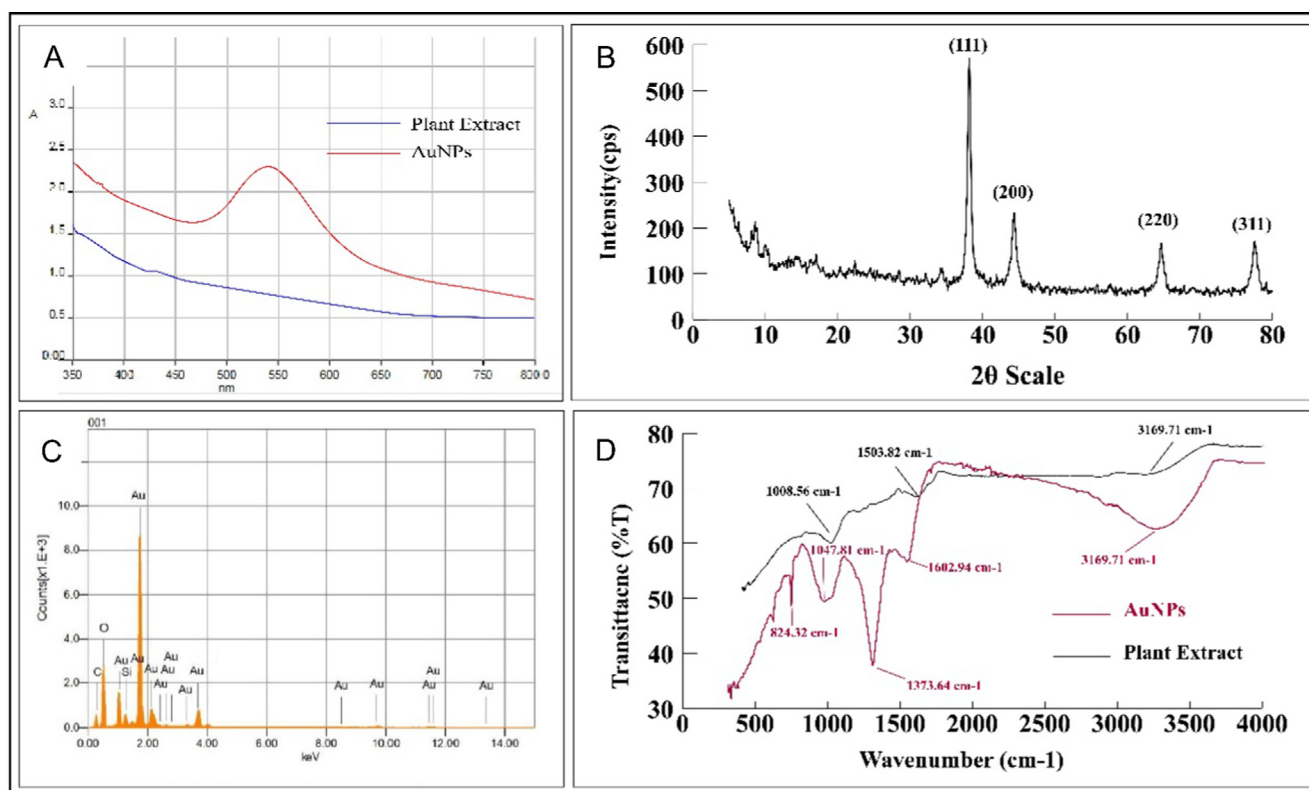
Fig. 2 (A) UV–visible spectra, (B) Energy dispersive spectra, (C) XRD pattern, (D) FT-IR spectrum of AuNPs and aqueous plant extract.

for 60 days at different intervals (15, 30, and 60 days). The SPR peak depicted that AuNPs had the best stability for the entire 60-day study period (Fig. 3D).

3.4. In vitro studies

3.4.1. Agar-well diffusion method

S. wightiana whole plant extract antibacterial activities were evaluated according to their IZ and MIC values against various bacterial strains (Table 1). AuNPs showed significant inhibitory zones against *E. coli* (25 mm), *S. epidermis* (23 mm), *S. enteritidis* (18 mm) and *S. typhi* (15 mm) with MIC values 0.13, 0.11, 0.16 and 0.12 mg/ml, respectively as compared to standard. These bacterial strains causes various infectious diseases such as UTI, travelers' diarrhea, prosthetic valve endocarditis (PVE), enteritidis and typhoid (Ya et al., 2017; Cogen et al., 2008). In folk medicines, the study plant is famous for the treatment of mentioned infectious disorders (Chashoo et al., 2012; Najamul et al., 2020; Niaz et al., 2019). According to published literature, phenolic compounds are mainly responsible for bactericidal activity (Araújo et al., 2014). *S. wightiana* contain different phytochemicals including phenolic, flavonoids, anthocyanins, quercetin and chlorogenic acid etc. (Najamul et al., 2020). Present study showed that AuNPs potentiated the antibacterial activity of crude extract against some of the studied pathogens thereby reducing the dose and side effects. Therefore, it is suggested that *S. wightiana* derived AuNPs can be further studied to develop effective remedy used against these pathogenic strains. It has been reported that membrane damage and toxicity occur due to the biophysical

interactions between AuNPs and bacteria through cellular uptake, aggregation and biosorption (Marwah et al., 2017). However, further research is needed to determine the specific mechanism for the same.

3.4.2. Agar slanting method

The zones of inhibition produced by plant extract, AuNPs and standard against various fungal strains are shown in Table 2. Among fungal strains *S. wightiana* derived AuNPs showed highest percent inhibition against *F. solani* (90%), *M. canis* (80%) and *A. terreus* (50%) with MIC values 0.02, 0.01 and 0.51 mg/ml, respectively as compared to standard. About half of human disease involving *Fusarium* is caused by *F. solani*. *Fusarium* species are widely distributed in the environment and are capable of causing a number of human infections including localized superficial (keratitis and skin infections), subcutaneous and disseminated infections (Laura et al., 2021). This is the most common opportunistic filamentous fungus after *Aspergillus* spp. and is highly resistant to most antifungal agents (Jain et al., 2011). In present study, AuNPs showed significant activity against the said fungi. In addition, the plant is famous for the treatment of disseminated and skin related infection. Therefore, *S. wightiana* derived AuNPs can be considered as an effective alternative therapy for the treatment of above mentioned disorders. According to the literature, antifungal drugs' possible mechanisms may include inhibition of cell wall synthesis and the formation of pores (Kaur et al., 2021). However, it is important to find out the exact mechanism for the studied NPs to come to a definite conclusion.
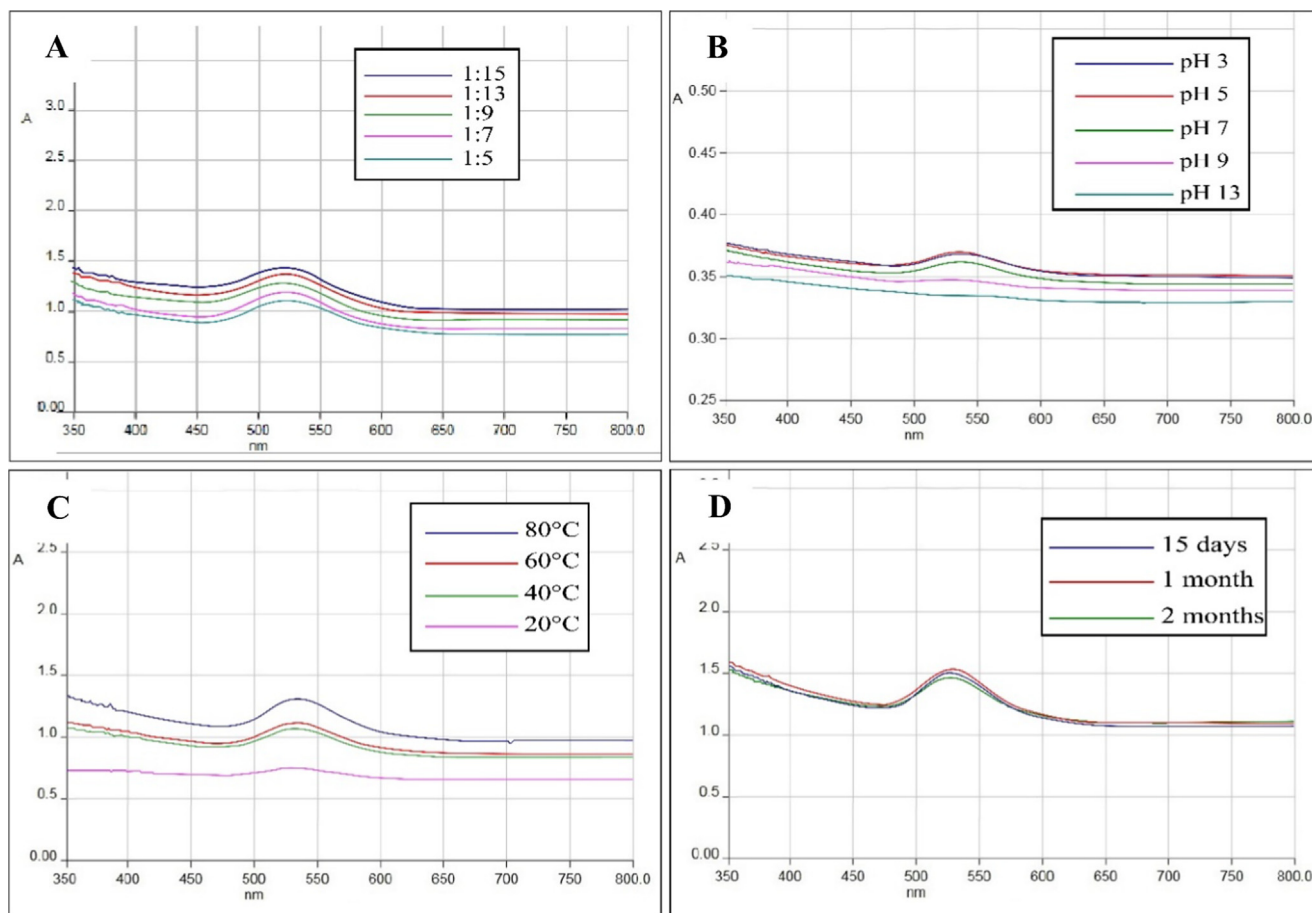
Fig. 3 (A) UV–Vis absorption spectra of AuNPs at different concentration of gold salt; (B) pH; (C) temperature and (D) at different time interval.

Table 1 IZ and MIC of extract, AuNPs and standard against different bacterial strains.

Bacterial strains	Extract		AuNPs		Std.	
	IZ	MIC	IZ	MIC	IZ	MIC
Bacillus subtilis	–	–	–	–	36	0.0002
Escherichia coli	14	0.69	25	0.13	13	0.0003
Klebsiella pneumonia	–	–	–	–	16	0.0014
Pseudomonas aeruginosa	–	–	–	–	32	0.0023
Salmonella enteritidis	14	0.66	18	0.16	31	0.0012
Salmonella typhi	10	0.81	15	0.12	33	0.0004
Shigella flexneri	–	–	–	–	35	0.0017
Staphylococcus aureus	–	–	–	–	30	0.0017
Staphylococcus epidermis	13	0.35	23	0.11	29	0.0016

IZ: Inhibition zone (mm); MIC: mg/ml; Std. Imipenem.

3.4.3. Cyclooxygenase (COX-2) and 5-lipoxygenase (5-LOX) assay

COX-2 and 5-LOX enzymes were inhibited by both extract and AuNPs in a concentration-dependent manner (Table 3). The IC$_{50}$ of AuNPs were 30.64 and 17.27 µg/ml, compared to Montelukast (25.96 µg/ml) and Celecoxib (14.18 µg/ml) for 5-LOX and COX-2 enzymes, respectively. Previously, several COX-2 or 5-LOX enzyme inhibitors have been developed as anti-inflammatory drugs (Viji and Helen, 2008). In our study AuNPs significantly inhibited both the enzymes thereby showing a strong potential to be developed as anti-inflammatory drug.

3.4.4. Antioxidant activity

The DPPH radical scavenging activity of the extract, AuNPs and standard are shown in Table 4. It demonstrated concentration dependent activity of AuNPs and extract with IC$_{50}$ value 37.23 and 43.65 µg/ml, respectively compared to that of

Table 2 IZ and MIC of extract, AuNPs and standard against different fungal strains.

Fungal strains	Extract		AuNPs		Std.	
	IZ	MIC	IZ	MIC	IZ	MIC
Alternaria alternata	40	0.61	40	0.81	100	0.0002
Aspergillus flavus	–	–	–	–	100	0.0014
Aspergillus niger	30	0.78	40	0.75	100	0.0030
Aspergillus terreus	30	0.65	50	0.51	100	0.0003
Candida albicans	–	–	–	–	100	0.0015
Candida glabrata	–	–	–	–	100	0.0015
Fusarium solani	30	0.80	90	0.02	100	0.0002
Microsporum canis	40	0.45	80	0.01	100	0.0003
Trichophyton longifusis	–	–	–	–	100	0.0008

IZ: Inhibition zone (%); MIC: mg/ml; Std. Miconazole.

Table 3 The relative % inhibition of COX-2 and 5-LOX enzymes by extract, AuNPs and standards.

	% Inhibition					
Concentration (µg/ml)	Extract		AuNPs		Celecoxib	Montelukast
	COX-2	5-LOX	COX-2	5-LOX	COX-2	5-LOX
15.6	5.25 ± 0.55	6.25 ± 0.80	12.70 ± 1.37	14.30 ± 1.20	14.30 ± 1.20	17.30 ± 1.45
31.25	15.55 ± 1.25	18.45 ± 1.85	39.0 ± 4.16	40 ± 2.89	41.70 ± 4.41	40.0 ± 2.89
62.5	24.34 ± 2.55	28.65 ± 2.25	45.80 ± 3.40	48.80 ± 3.90	51.40 ± 3.60	48.70 ± 3.93
125	30.25 ± 3.12	32.80 ± 4.40	56.30 ± 4.70	50.30 ± 2.60	59.30 ± 6.50	55.80 ± 4.96
250	35.50 ± 2.90	35.75 ± 3.55	66.50 ± 2.96	58.30 ± 3.40	68.80 ± 3.55	65.30 ± 2.91
500	41.55 ± 4.45	44.0 ± 4.0	69.0 ± 5.58	63.50 ± 4.40	70.95 ± 2.60	70.0 ± 4.05
1000	45.60 ± 3.70	47.80 ± 3.50	75.0 ± 4.89	71.90 ± 5.45	83.30 ± 5.73	76.70 ± 5.40
IC_{50} µg/ml	25.23	37.35	17.27	30.64	14.18	25.96

Table 4 DPPH free radical scavenging activity of extract, AuNPs and standard.

Concentrations (µg/ ml)	% Scavenging activity		
	Extract	AuNPs	Ascorbic acid
15.6	4.23 ± 0.80	10.7 ± 1.20	12.3 ± 1.45
31.25	13.52 ± 1.10	29.7 ± 4.06	34.7 ± 3.53
62.5	19.56 ± 2.45	39.3 ± 5.46	44.7 ± 5.04
125	23.89 ± 4.56	44.8 ± 6.89	50.0 ± 6.03
250	31.21 ± 4.56	49.3 ± 6.03	54.8 ± 7.84
500	37.78 ± 5.67	56.0 ± 1.53	60.0 ± 5.77
1000	41.34 ± 3.22	68.7 ± 3.76	77.8 ± 4.10
IC_{50} (µg/ ml)	43. 65	37.23	31.56

standard (31.56 µg/ml). Free radicals are highly reactive and toxic substances that causes several health problems including cancer, diabetes, aging, cardiovascular disorders, atherosclerosis and liver cirrhosis (Abdulrahman et al., 2021; Miki et al., 2021). The synthesized AuNPs and extract showed promising antioxidant activity therefore it is suggested that the study plant may be further studied for the mentioned pathological conditions.

3.5. In vivo studies: anti-inflammatory and analgesic activities

3.5.1. Carrageenan-induced paw edema

AuNPs showed significant anti-inflammatory activity ($P \leq 0.001$) at 10 and 20 mg/kg, compared to standard (Table 5). The maximum inhibition (43.70, 48.80 and 57.08%) was shown at 20 mg/kg dose at both early and late hours of inflammation as compared to standard which showed 51.96, 60.81 and 74.49% inhibition at the same dose. Crude extract showed similar activity but at higher dose of 200 mg/kg. At all test doses, both the extract and the AuNPs demonstrated dose-dependent activity.

In present study, the carrageenan induced paw edema model showed biphasic response. Several mediators are released during the early phase of inflammation including serotonin and histamine while its later phase is accompanied by the release of neutrophil derived mediators, free radicals and eicosanoid. Bradykinin and prostaglandin etc. are produced in between the early and late phase and are responsible for the formation of inflammatory exudates (Ihsan et al., 2021). AuNPs were found effective in both the phases.

NSAIDs are commonly prescribed for the mitigation of pain and inflammatory conditions such as osteoporosis and rheumatoid arthritis. However, because these drugs are mostly associated with peptic ulcer and other GI disorders, attention has been paid to alternative therapies. The results of the study suggests that *S. wightiana* might be effective in the treatment of

Table 5 Anti-inflammatory effect of plant extract, AuNPs and standard on paw edema induced by carrageenan in mice.

Groups	Mean change in the hind paw volume (ml)				
	Dose (mg/kg)	BV	1 h	3 h	5 h
Control	–	0.11 ± 0.021	0.254 ± 0.002	0.250 ± 0.011	0.247 ± 0.002
Extract	50	0.10 ± 0.030	0.221 ± 0.003[a] (12.99)[d]	0.198 ± 0.020[a] (20.80)	0.188 ± 0.003[a] (23.88)
	100	0.09 ± 0.020	0.211 ± 0.005[a] (16.92)	0.190 ± 0.003[a] (24.53)	0.171 ± 0.005[b] (30.76)
	200	0.13 ± 0.020	0.183 ± 0.004[b] (27.95)	0.150 ± 0.001[b] (40.0)	0.129 ± 0.001[c] (47.77)
AuNPs	5	0.09 ± 0.022	0.198 ± 0.0051[a] (22.04)	0.170 ± 0.001[b] (32.01)	0.165 ± 0.004[a] (33.19)
	10	0.11 ± 0.032	0.159 ± 0.006[b] (37.40)	0.141 ± 0.001[b] (43.60)	0.126 ± 0.006[c] (48.98)
	20	0.12 ± 0.012	0.143 ± 0.004[c] (43.70)	0.128 ± 0.004[c] (48.80)	0.106 ± 0.004[c] (57.08)
Diclofenac	20	0.10 ± 0.02	0.122 ± 0.005[c] (51.96)	0.098 ± 0.004[c] (60.81)	0.063 ± 0.002[c] (74.49)

Data is expressed as mean ± SEM (n = 5) and analyzed by one way ANOVA followed by Dunnet post hoc test using GraphPad Prism 5; BV = basal volume; [c]$P \leq 0.001$, [b]$P \leq 0.01$, [a]$P \leq 0.05$; [d]Values in parentheses indicate % inhibition.

inflammation and pain. It has been documented that flavonoids and phenolic compounds are the major constituents in combating different microbes, pain and inflammation. Besides their antioxidant activity, they are also responsible for inhibition of different pathways including COX-2 and 5-LOX (Duangjai et al., 2018; Panche et al., 2016). As it has been mentioned previously that the study plant is famous for the treatment of a variety of pathological conditions including pain and inflammation; the added advantage of AuNPs may potentiate its effect against the same. As a result, AuNPs may be considered as a safe and effective alternative herbal therapy for the treatment of these pathological conditions.

3.5.2. Hot plate test (central analgesic activity)

AuNPs showed significant ($P \leq 0.001$) dose dependent protective effect with maximum inhibition (56.22%) at 20 mg/kg. Tramadol showed a significant ($P \leq 0.001$) analgesic activity with maximum inhibition (66.55%) at 20 mg/kg. The crude extract demonstrated maximum inhibition activity (35.31%) at the highest test dose (200 mg/kg). At 60 min. of total study duration, all test agents demonstrated maximum inhibition (Table 6).

The method used in this study is useful for evaluating the activity of centrally acting analgesics, which are used to elevate the pain threshold via activating the opioid receptors. The activation of these receptors is associated with spinal as well as peripheral analgesia (Mohamad et al., 2017). Results of the study suggest that the extract is a centrally acting analgesic and therefore may be considered in the development of potentially safe and effective therapy.

4. Conclusion

In this study, the whole plant extract of S. wightiana was used for simple, rapid and environment friendly synthesis of AuNPs. Different analytical techniques i.e. UV–Vis spectroscopy, XRD, TEM, SEM, EDX, FTIR and zetasizer were used for its characterization. Their average size was in the range 10–50 nm. SEM and TEM techniques revealed the formation of heterogeneously dispersed nanoparticles; the common shapes observed were trigonal, cubic and hexagonal. The AuNPs showed significant antimicrobial activity against E. coli, S. epidermis, F. solani and M. canis. It showed significant anti-inflammatory activity at both early and late hours of inflammation. In vitro model depicted concentration dependent inhibition of both 5-LOX and COX-2 enzymes. The AuNPs revealed good antioxidant activity against common free radicals i.e. DPPH. Similarly, they exhibited dose dependent analgesic effect. The findings suggest that AuNPs should be evaluated further in order to develop more effective and safe formulations.

Table 6 Effect of plant extract, AuNPs and standard on hot plate-induced pain in mice.

Groups	Dose (mg/kg)	30 min	60 min	90 min
Control	–	8.34 ± 0.32	9.67 ± 0.23	10.11 ± 0.22
Extract	50	10.94 ± 0.21 (12.0%)[d]	13.89 ± 0.32[a] (20.75%)	12.98 ± 0.22 (14.42%)
	100	13.10 ± 0.23 (21.97%)	15.90 ± 0.4[a] (30.64%)	14.83 ± 0.25 (23.74%)
	200	14.80 ± 0.43[b] (29.91%)	16.85 ± 0.32[b] (35.31%)	15.40 ± 0.20[a] (26.54%)
AuNPs	5	14.02 ± 0.44[a] (26.22%)	16.63 ± 0.43[a] (34.23%)	16.19 ± 0.76[a] (30.56%)
	10	15.98 ± 0.54[b] (35.27%)	19.55 ± 0.52[c] (48.59%)	17.45 ± 0.51[b] (36.90%)
	20	18.52 ± 0.52[c] (46.99%)	21.10 ± 0.65[c] (56.22%)	20.65 ± 0.58[c] (52.99%)
Tramadol	20	20.10 ± 0.72[c] (54.29%)	23.20 ± 0.35[c] (66.55%)	22.20 ± 0.69[c] (60.78%)

Data is expressed as mean ± SEM (n = 5) and analyzed by one way ANOVA followed by Dunnet post hoc test using GraphPad Prism 5; [a]$P \leq 0.05$, [b]$P \leq 0.01$, [c]$P \leq 0.001$; [d]Values in parentheses indicate % inhibition.

Declaration of Competing Interest

The authors declare that they have no known competing financial interests or personal relationships that could have appeared to influence the work reported in this paper.

Appendix A. Supplementary material

Supplementary data to this article can be found online at https://doi.org/10.1016/j.arabjc.2021.103343.

References

Abdulrahman, A.A., Essam, A.T., Nageeb, A.A., Abdul, W.A.K., Mohamed, A., Deyala, M.N., 2021. Phytochemical components, antioxidant and anticancer activity of 18 major medicinal plants in Albaha region, Saudi Arabia. Biocatal. Agric. Biotechnol. 34, 102020. https://doi.org/10.1016/j.bcab.2021.102020

Ahmad, A., Wei, Y., Ullah, S., Shah, S.I., Nasir, F., Shah, A., Iqbal, Z., Tahir, K., Khan, U.A., Yuan, Q., 2017. Synthesis of phytochemicals-stabilized gold nanoparticles and their biological activities against bacteria and Leishmania. Microb. Pathog. 110, 304–312. https://doi.org/10.1016/j.micpath.2017.07.009.

Ahmad, S.I., Ali, G., Muhammad, T., Ullah, R., Umar, M.N., Hashmi, A.N., 2020. Synthetic β-hydroxy ketone derivative inhibits cholinesterases, rescues oxidative stress and ameliorates cognitive deficits in 5XFAD mice model of AD. Mol. Biol. Rep. 47 (12), 9553–9566. https://doi.org/10.1007/s11033-020-05997-0.

Alaa, A.A.A., Yazan, A., Mazhar, S.A.Z., Khalid, M.A., Bahaa, A., Osama, A.A., Alaaldin, M.A., Mourad, B., David, J.E., 2018. Synthesis of gold nanoparticles using leaf extract of Ziziphus zizyphus and their antimicrobial activity. Nanomaterials 8, 174. https://doi.org/10.3390/nano8030174.

Araújo, A.A., Soares, L.A.L., Assunção Ferreira, M.R., Souza Neto, M.A., Silva, G.R., Araújo, R.F., Guerra, G.C.B., Melo, M.C.N., 2014. Quantification of polyphenols and evaluation of antimicrobial, analgesic and anti-inflammatory activities of aqueous and acetone– water extracts of Libidibia ferrea. Parapiptadenia rigida and Psidium guajava J. of Ethnopharmacol. 156, 88–96. https://doi.org/10.1016/j.jep.2014.07.031.

Boyanova, L., Gergova, G., Nikolov, R., Derejian, S., Lazarova, E., Katsarov, N., Mitov, I., Krastev, Z., 2005. Activity of Bulgarian propolis against 94 Helicobacter pylori strains in vitro by agar-well diffusion, agar dilution and disc diffusion methods. J. Med. Microbiol. 54, 481–483. https://doi.org/10.1099/jmm.0.45880-0.

Chashoo, I.A., Dinesh, K., Bhat, Z.A., Khan, N.A., Vijender, K., Javaid, A.N., 2012. Antimicrobial studies of Sambucus wightiana Wall. ex. Wight & Arn. J. Pharm. Res. 5 (5), 2467–2468. https://doi.org/10.13140/RG.2.2.14619.36646.

Cogen, A.L., Nizet, V., R.L., Gallo., 2008. Skin microbiota: a source of disease or defence? Br. J. Dermatol. 158 (3), 442–455. doi: 10.1111/j.1365-2133.2008.08437.x

Dan, Z., Xin-lei, M., Yan, G., He, H., Guang-wei, Z., 2020. Green synthesis of metallic nanoparticles and their potential applications to treat cancer. Front. Chem. 8, 799. https://doi.org/10.3389/fchem.2020.00799.

Duangjai, T., Areeya, T., Apinan, P., Aujana, Y., 2018. Flavonoids and Other Phenolic Compounds from Medicinal Plants for Pharmaceutical and Medical Aspects: An Overview Medicines (Basel). 5 (3), 93. doi: 10.3390/medicines5030093

Elechiguerra, J.L., Reyes-Gasga, J., Yacaman, M.J., 2006. The role of twinning in shape evolution of anisotropic noble metal nanostructures. J. Mater. Chem. 16, 3906–3919. https://doi.org/10.1039/B607128G.

Eloff, J., 1998. A sensitive and quick microplate method to determine the minimal inhibitory concentration of plant extracts for bacteria. Planta Med. 64 (08), 711–713. https://doi.org/10.1055/s-2006-957563.

Fazli, K., Zafar, I., Ayub, K., Zakiullah, Fazli, N., Khan, Muhammad, S.K., 2012. Validation of some of the ethnopharmacological uses of xanthium strumarium and duchesnea indica. Pak. J. Bot. 44, 1199-1201.

Ilahi, I., Fazli, K., Umar, K.S., Alghamdi, S., Ullah, R., Zaki, U., Dablool, A.S., Alam, M., Ayub, K., Atif, A.K.K., 2021. Synthesis of silver nanoparticles using root extract of Duchesnea indica and assessment of its biological activities. Arab. J. Chem. 14 (5), 103110. https://doi.org/10.1016/j.arabjc.2021.103110.

Jain, P.K., Gupta, V.K., Misra, A.K., Gaur, R., Bajpai, V., Issar, S., 2011. Current status of Fusarium infection in human and animal. Asian. J. Anim. Vet. Adv. 6 (3), 201–227. https://doi.org/10.3923/ajava.2011.201.227.

Kar, X.L., Kamyar, S., Yen, P.Y., Sin-Yeang, T., Hossein, J., Roshanak, R.M., Thomas, J.W., 2020. Recent developments in the facile bio-synthesis of gold nanoparticles (AuNPs) and their biomedical applications. Int. J. Nanomed. 15, 275–300. https://doi.org/10.2147/IJN.S233789.

Kaur, N., Bains, A., Kaushik, R., Dhull, S.B., Melinda, F., Chawla, P., 2021. A review on antifungal efficiency of plant extracts entrenched polysaccharide-based nanohydrogels. Nutrients 13, 2055. https://doi.org/10.3390/nu13062055.

Khafsa, M., Mushtaq, A., Guolin, Z., Neelam, R., Muhammad, Z., Shazia, S., Syed, N.S., 2018. Traditional plant based medicines used to treat musculoskeletal disorders in Northern Pakistan. Eur. J. Integr. Med. 19, 17–64. https://doi.org/10.1016/j.eujim.2018.02.003.

Laura, B.D., Carla, W., Lara, B.I., Paula, C.S., Janio, M.S., 2021. Activity of MSI-78, h-Lf1- 11 and cecropin B antimicrobial peptides alone and in combination with voriconazole and amphotericin B against clinical isolates of Fusarium solani. J. Med. Mycol. 31 (2), 101119. https://doi.org/10.1016/j.mycmed.2021.101119

Lingadurai, S., Nath, L.K., Kar, P.K., Besra, S.E., Joseph, R.V., 2007. Anti-inflammatory and anti- nociceptive activities of methanolic extract of the leaves of Fraxinus floribunda Wallich. Afr. J. Tradit. Complement. Altern. Med. 4 (4), 411–416. https://doi.org/10.4314/ajtcam.v4i4.31235.

Lydia, D.E., Ameer, K., Immanuel, P., Galal, A.E., Naif, A., Mariadhas, V.A., 2020. Photo- activated synthesis and characterization of gold nanoparticles from Punica granatum L. seed oil: An assessment on antioxidant and anticancer properties for functional yoghurt nutraceuticals. J. Photochem. Photobiol. B 206,. https://doi.org/10.1016/j.jphotobiol.2020.111868 111868.

Marwah, M.M., Shereen, A.F., Hisham, A.E., Gina, M.M., Taher, A.S., 2017. Antibacterial effect of gold nanoparticles against Corynebacterium pseudotuberculosis. Int. J. Vet. Sci. Med. 5 (1), 23–29. https://doi.org/10.1016/j.ijvsm.2017.02.003.

Miki, G., Gretty, K.V., Ana, A.K., 2021. Evaluation of the antioxidant activities of aqueous extracts from seven wild plants from the Andes using an in vivo yeast assay. Results Chem. 3,. https://doi.org/10.1016/j.rechem.2021.100098 100098.

Mohamad, A.H., Ahmed, E., Maha, A., Abdalla, E., 2017. Evaluation of analgesic activity of Papaver libanoticum extract in mice: involvement of opioids receptors. Evid. Based Complement. Alternat. Med. 2017, 13. https://doi.org/10.1155/2017/8935085.

Mudasir, A.M., Zahoor, D., Mani, P., Waseem, B., Rao, M.V., 2018. In-vitro anti-proliferative activity of Sambucus wightiana. J. Pharmacogn. Phytochem. 7 (3), 3282–3283.

Muhammad N., Bilal, H.A., Muhammad, Y., Waqar, A., Taimoor, K., 2017. A review of the green syntheses and anti-microbial applications of gold nanoparticles. Green. Chem. Lett. Rev.10,216-227. https://doi.org/10.1080/17518253.2017.1349192

Najamul, H., Hamidullah, S., Muhammad, J., Sajjad, A.S., Shah, F., Abdullah, Muhammad, T.A., Adil, K., Imran, U., Muhammad, A. K., Faheem, J., Muhammad, W., Sajid, I., Mahmood, K., 2020. Antimicrobial activity and biomedical application of sambucus wightiana phenolic extract against gram positive and gram-negative strains of bacteria. J. Biomed. Sci. 9 (3), 12. DOI: 10.36648/2254-609X.9.3.12.

Niaz, M., Shafiq, A.T., Altaf, A.M., Fazli, K., Maria, Q., Muhammad, A.S., Shumaila, P., Ali, S., Abid, A., Tahseen, A.C., 2019. Evaluation of the screening and isolation of total flavonoids of Sambucus wightiana (TFSW) for its analgesic activity in albino mice. Adv. Biores. 10 (4), 124–131. https://doi.org/10.15515/abr.0976-4585.10.4.124131.

Niu, W., Xu, G., 2011. Crystallographic control of noble metal nanocrystals. Nanotoday. 6 (3), 265–285. https://doi.org/10.1016/j.nantod.2011.04.006.

Okur, M.E., Karadag, A.E., Ozhan, Y., Sipahi, H., Ayla, S., Daylan, B., Kultur, S., Demirci, B., Demirci, F., 2021. Anti-inflammatory, analgesic and in vivo-in vitro wound healing potential of the Phlomis rigida Labill. extract. J. Ethnopharmacol. 266,. https://doi.org/10.1016/j.jep.2020.113408 113408.

Olomola, T.O., Mphahlele, M.J., Gildenhuys, S., 2020. Benzofuran selenadiazole hybrids as novel a-glucosidase and cyclooxygenase-2 inhibitors with antioxidant and cytotoxic properties. Bioorg. Med. Chem. 100, 103945. https://doi.org/10.1016/j.bioorg.2020.10395.

Panche, A.N., Diwan, A.D., Chandra, S.R., 2016. Flavonoids: an overview. J. Nutr. Sci. 5,. https://doi.org/10.1017/jns.2016.41 e47.

Suh, I.K., Ohta, H., Waseda, Y., 1988. High-temperature expansion of six metallic elements measured by dilatation method and X-ray diffraction. J. Mater. Sci. 23, 757–760. https://doi.org/10.1007/BF01174717.

Sundus, J.A., Bin, G., 2020. A review on the synthesis and functionalization of gold nanoparticles as a drug delivery vehicle. Int. J. Nanomedicine. 15, 9823–9857. https://doi.org/10.2147/IJN.S279094.

Tejasvi, S., Athira, J., Mohammad, A., Asha, A.M., 2021. Green synthesized gold nanoparticles with enhanced photocatalytic activity. Mater. Today. 42 (2), 1166–1169. https://doi.org/10.1016/j.matpr.2020.12.531.

Tokeer, A., Irshad, A.W., Irfan, H.l., Aparna, G., Nikhat, M., Aijaz, A., Jahangeer, A., Ayed, S.A., 2013. Antifungal activity of gold nanoparticles prepared by solvothermal method. Mater. Res. Bull. 48(1),12-20. https://doi.org/10.1016/j.materresbull.2012.09.069

Viji, V., Helen, A., 2008. Inhibition of lipoxygenases and cyclooxygenase-2 enzymes by extracts isolated from Bacopa monniera (L.) Wettst. J. of Ethnopharmacol. 118 (2), 305–311. https://doi.org/10.1016/j.jep.2008.04.017.

Winter, C.A., Risley, E.A., Nuss, G.W., 1962. Carrageenin-induced Edema in hind paw of the rat as an assay for antiinflammatory drugs. Proc. Soc. Exp. Biol. Med. 111 (3), 544– 547. https://doi.org/10.3181/00379727-111-27849.

Ya, H., Na, Y., Xiumin, W., Da, T., Ruoyu, M., Xiao, W., Zhanzhan, L., Jianhua, W., 2017. Killing of Staphylococcus aureus and Salmonella enteritidis and neutralization of lipopolysaccharide by 17-residue bovine lactoferricins: improved activity of Trp/Ala-containing molecules. Sci. Rep. 7, 44278. https://doi.org/10.1038/srep44278.